Soft Matter

Accepted Manuscript

ROYAL SOCIETY OF CHEMISTRY

www.rsc.org/softmatter

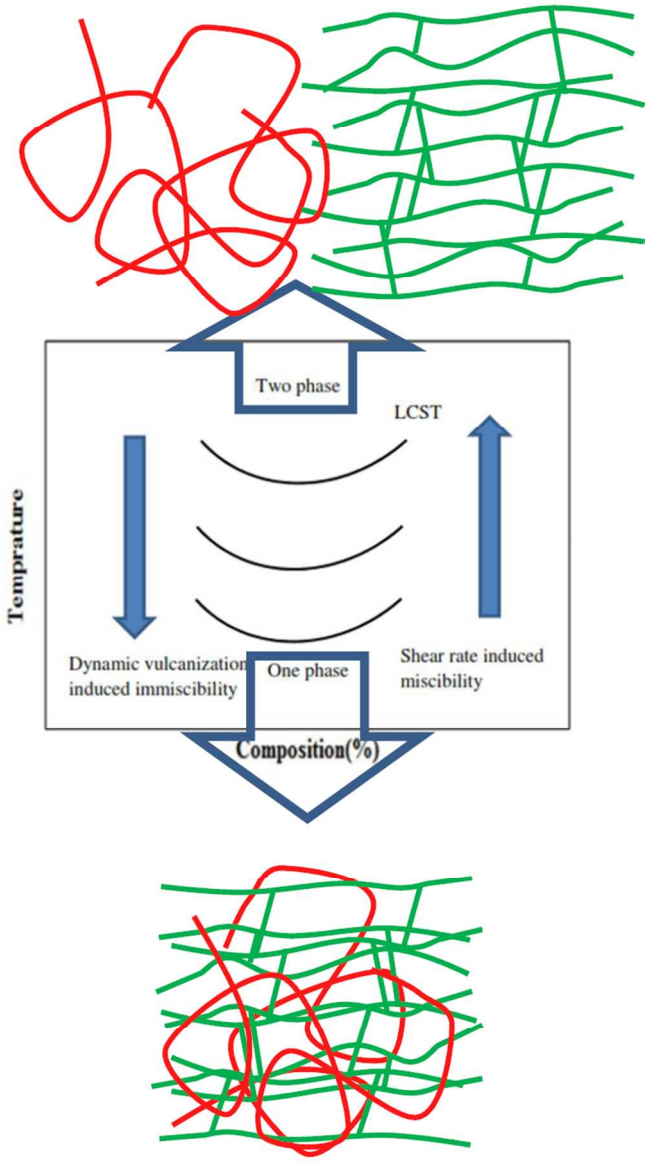

222x385mm (96 x 96 DPI)

Does dynamic vulcanization induce phase separation?*

Mohammad Mahdi Abolhasani[†a],Fatemeh Zarejousheghani[a], Minoo Naebe[b], Qipeng Guo[b]

[a]Chemical Engineering Department, University of Kashan, Kashan, Iran

[b]Institute for Frontier Materials, Deakin University, VIC 3216, Australia

Abstract

Immiscible and miscible blends of poly(vinylidene fluoride) (PVDF) and acrylic rubber(ACM) were subjected to dynamic vulcanization to investigate the effect of crosslinking in phase separation. As a result of different processability, mixing torque behavior of miscible and immiscible blends was significantly different from one another. Scanning electron microscopy (SEM) was used to investigate the morphology of the system. After dynamic vulcanization, submicron ACM droplets were observed for the samples near the binodal curve of the system in mixing condition. Small angel X-ray scattering (SAXS) and differential scanning calorimetry (DSC) analysis were used to investigate the effect of dynamic vulcanization on lamellar structure of the system. It was shown that for samples near the boundary of phase separation, increasing the crosslink density led to decrease in lamellar long period (L) as a sign of increment of crosslink density induced phase decomposition. Effects of shear rate on the final morphology of the system were investigated by changing the mixing temperature and by comparing the results of dynamic vulcanization at one phase and two phase regions.

Keywords: Dynamic vulcanization, Phase separation, crosslink density, morphology

* Paper dedicated to Professor Hossein Nazokdast from Amirkabir University of Technology on the occasion of his 70th birthday.

† To whom correspondence should be addressed. E-mail: abolhasani@kashanu.ac.ir

1. Introduction

Miscible blends containing a crystallizable component have attracted considerable interest. However, little attention has been paid to miscible or even partially miscible blends containing one vulcanizable rubber with a crystallizable linear polymer (1-7). From a thermodynamics point of view, an increase in the molecular weight of either of the components of a miscible blend should reduce the entropy of mixing. Consequently, phase separation induced by cross-linking is expected for systems with a positive (endothermic) enthalpy of mixing (1, 4).

An important method to improve the elastomeric properties and processability of the thermoplastics is the dynamic vulcanization of the rubber phase in the presence of a suitable crosslinking agent, during the melt mixing with the thermoplastics, giving rise to a thermoplastic vulcanizate(TPV). This technique has been employed in the development of several TPVs (8-15). We have published a series of investigations on the effect of curing on miscibility of thermosetting polymer blends(2-6). The hydrogen-bonding interaction was considered to be the driving forces for cure induced miscibility, and it is responsible for the favorable exothermic heat of mixing that is the thermodynamic basis of the miscibility in studied systems.

Kyu et al.(16) studied effect of vulcanization on miscibility of syndiotactic polypropylene/ethylene propylene diene monomer (M-class) rubber (sPP/EPDM) blends. In contrary to Guo et al.(2-6) they showed that curing reaction induced phase separation in this blend. In these studies, static vulcanization have been extensively used and less attention has been paid to dynamic vulcanization of miscible polymer blends. Li et al.(1) investigated dynamic vulcanization of PVDF/ACM 50/50 blend and showed that vulcanization indeed induce phase separation. They assumed that after vulcanization this blend is still miscible in the melt state but after cooling to room temperature, PVDF and ACM have been phase separated. No phase diagram was presented for this blend and no further investigation provided to confirm this assumption.

The complicated interrelationship between phase behavior and crosslinking in vulcanizable miscible blends containing one crystallizable component has not yet been realized. Furthermore, it is expected that crosslinking will affect the crystallization of the blend.

PVDF is a semicrystalline polymer which is miscible with many polymers containing carbonyl group, such as polyacrylates (17-22), poly acetates (23) and polyketone (24) as a result of specific interactions of CF_2 dipoles with carbonyl group. Acrylic rubber is a copolymer of ethyl acrylate with a minor amount (5%w) of chlorine cure-site.

In our previous paper, miscibility of PVDF/ACM blend has been investigated(18, 19) by plotting the phase diagram of this blend (Figure1). We found that PVDF and ACM are miscible in ACM rich blends and in the blends with more than 50% PVDF content. The binodal and equilibrium melting point curves intersect at about 173ºC. The main advantage of this blend is the ability of PVDF to crystalize even in ACM rich blends in contrary to many miscible blends containing PVDF (25, 26).

While studies into static curing of miscible thermosetting resins have been widely reported, no studies on dynamic vulcanization of thermoplastics have been conducted. Here, we report the results of our investigation on dynamic vulcanization of PVDF/ACM blends and will explore the effects of dynamic vulcanization on phase diagram, morphology and crystalline structure of this polymer blend system.

2. Experiments

2.1. Materials and methods

PVDF (Kynar 710;Mw=70000, Mw/Mn=2) from Arkema and acrylic rubber (Grade AR71;Mw=620000, Mw/Mn=9) from Zeon Advanced Polymix Co.(Thailand) were used in this work. The major component of the acrylic rubber was poly (ethyl acrylate) (PEA), which contains a small amount (5%w) of chlorine cure-site monomer. All polymers were dried in a vacuum oven at 80˚C for at least 12h before processing. The blends without adding curative were prepared using a Brabender type plastic mixer with a two rotors at a rotation speed of 100rpm at 190˚C for 10min. For dynamic vulcanization, curing agents sodium

stearate(5phr), magnesium oxide (10phr) and various amounts of sulfur were added after mixing of PVDF and ACM for 10 min. Samples then were hot pressed into the films at 200˚C and allowed to slowly cool down to room temperature. Table 1. shows details of samples prepared for this study.

2.2. Characterization

Differential Scanning Calorimetery (DSC) was performed using a TA Instrument Q200 under nitrogen flow at a heating rate of 10°C/min. Crystallinity (Xc) was measured during the heating, on the basis of the heat of fusion of 105J/g for a 100% crystalline PVDF.

The morphology and microstructure of samples was examined by scanning electron microscopy (SEM), Leica S440 equipment. Samples were cryogenically fractured in liquid nitrogen and then sputter-coated with a thin layer of gold prior to imaging.

Small-angle X-ray scattering (SAXS) experiments were conducted at the Australian Synchrotron on the small/wide angle X-ray scattering beam-line utilizing an undulator source that allowed measurement at a very high flux to moderate scattering angles (hs) and a good flux at the minimum scattering vector (q) limit (0.012 nm^{-1}). The intensity profiles were interpreted as the plot of scattering intensity (I) versus q:

$$q = (4/\lambda) \sin(\theta/2) \quad (1)$$

where λ is the wavelength and is equal to 0.062 nm. The scattering invariant, Q, was determined from the total integrated intensity, I(q) using (27):

$$Q = \int I(q).q^2 dq \quad (2)$$

The one-dimensional electron density correlation function was obtained from (28):

$$\gamma(x) = \frac{\int I(q).q^2 \cos(qx) dq}{Q} \quad (3)$$

where x is a dimension along the normal to the lamellar stacks. Parameters such as the long period, L, average crystalline thickness, l_c and amorphous layer thickness, l_a, were determined using the method of Strobl and Schneider (28).

3. Results

3.1. Dynamic vulcanization and Melt processability

Figure 2. shows the mixing torque vs. mixing time for dynamically vulcanized samples with 1phr sulfur in the batch mixer. Note that curatives were added after a 10 minute of melt mixing of ACM and PVDF. A large increase in mixing torque of immiscible blends (blends with more than 50% PVDF), is observable after addition of curatives while miscible blends (blends with less than 50% PVDF) final mixing torque is even lower than the original blends torque. Immiscible blends performance is a common dynamic vulcanization behavior of TPVs reported repeatedly in the literature(8-15).

After dynamic vulcanization immiscible blends were melt processable whereas miscible blends were not. We were unable to hot press miscible blends and prepare a film. Vulcanization of miscible blends produced yellowish porous samples without any mechanical strength and structural integrity. Figure 3. shows the photographs of 80/20-C1, 50/50-C3, 50/50-C1/220, 50/50-C2, 20/80-C1 and 20/80-C3 after dynamic vulcanization. Efforts to prepare dog-bone shape samples from miscible dynamically vulcanized samples were unsuccessful while immiscible dynamically vulcanized samples readily hot pressed to films to prepare doge-bone test specimen. To better explain the observed phenomenon one should investigate the effects of dynamic vulcanization on phase separation. Therefore, analyses of effects of crosslink density on the miscible blends crystalline structure were conducted.

Figure 4. shows mixing torque values of 50/50, 40/60 and 20/80 miscible blends vulcanized by 1, 2 and 3phr sulfur to increase the crosslink density. 50/50 miscible blends showed an increase in mixing torque values by increasing the sulfur content while for other miscible samples' torques were insensitive to sulfur content. As shown in Figure3.b and 3.d, 50/50-C3 sample was completely melt processable with acceptable mechanical strength, but 50/50-C2 sample melt did not have enough consolidation to prepare dog-bone sample. Nonetheless, all other samples had yellowish color porous structure without any

structural integrity. As for 50/50-C3, sample torque and processability behavior were similar to immiscible TPVs.

3.2. Morphology of dynamically vulcanized PVDF/ACM blends.

Figure 5. shows the phase morphology of 80/20 immiscible blend, 50/50 and 20/80 miscible blends before and after dynamic vulcanization with 1phr sulfur. 80/20 immiscible blend clearly shows a matrix disperse morphology whereas miscible 50/50 and 20/80 blends have a smooth surface without any sign of inhomogeneity. However, morphology of these blends after dynamic vulcanization was completely different. 80/20-C1 sample showed a heterogeneous structure in which vulcanized rubber dispersed in PVDF matrix. On contrary, 50/50-C1 and 20/80-C1 samples showed a porous and coarse structure. The observed SEM images are absolutely coinciding to their melt processability and visual observation of these samples as shown in Figures 2 and 3, respectively.

Insets of Figure 5.d and 5.f show the morphology of dynamically vulcanized miscible samples with higher magnification. 50/50-C1 sample is full of ACM nano-phase separated droplets with diameters of less than 100nm while 20/80-C1 sample does not show any sign of phase separation. Since 50/50 sample phase composition is near the boundary of two phase region, Figure 1, it seems that vulcanization induce phase separation when the blend is not far into miscible region. Tang et al.(29) obtained a nanostructured thermoplastic vulcanizates by selectively crosslinking of ethylene vinyl acetate rubber (vinyl acetate (VA) content = 50 wt %) (EVM) and ethylene vinyl acetate copolymer.

Morphology of miscible samples with higher crosslink density was also investigated by SEM as shown in Figure 6. 50/50-C3 sample clearly shows a phase separated structure similar to immiscible samples as shown in Figure 6.a. This means that increasing the crosslink density increased the phase separation. Low magnification SEM image of the 40/60-C3 and 20/80-C3 shown in Figure 6.b and 6.c are completely alike to those with lower crosslink density; however, high magnification SEM images in inset of Figure 6. shows different morphology at nanoscale structure for these samples. Higher magnification SEM image of 40/60-C3 blend is similar to that of 50/50-C1 sample; nanometer droplets of ACM are phase separated

in the PVDF rich matrix. Nonetheless, increasing the crosslink density had no effects on morphology of 20/80 sample and SEM image of 20/80-C3 blend is similar to that of 20/80-C1 blend as shown in inset of Figure 6.c. A summary of torque status and morphology behavior of samples studied herein is presented in Table 2. While looking at results one may wonder why 50/50-C1and 40/60-C3 samples had nano-phase separated structure. Besides, when the curatives are added to the system the operating temperature of Brabender mixer is around 205ºC which is deep into two phase region for 50/50 and 40/60 blends (see Figure 1.) but why vulcanization behavior of these blends are similar to miscible blends? To explain these questions, a fresh 50/50-C1 sample was prepared where the mixer temperature set at 220ºC. From now on this sample is called 50/50-C1/220 (note that when the mixer temperature is set at 220°C, real temperature at mixing condition was 230-235°C). Figure 7. shows the mixing torque and SEM image for 50/50-C1/220 sample. After addition of curing agents mixing torque was increased and eventually leveled off which is associated to the processability of this sample. Dog-bone shaped specimen prepared from this sample, shown in inset of Figure 7.a, demonstrate the processability of this sample. SEM image of 50/50-C1/220 sample clearly shows the phase separated structure of the system which is different from morphology of the same sample prepared at 190ºC; ACM vulcanized droplets here are more than 400nm in diameter compared to 100nm droplets of 50/50-C1 sample. We will address the above mentioned questions and further explain some other unusual features of this complex system in the discussion section.

3.3. Miscibility and crystal structure of dynamically vulcanized PVDF/ACM blends

DSC thermograms of vulcanized and unvulcanized samples are presented in Figure 8. PVDF crystallinity for each sample was calculated from the heat of fusion during the first heating cycle. PVDF crystallinity is almost unaffected by blending with ACM, in contrary, crystallinity decreased with dynamic vulcanization and increment of crosslink density. However, a very broad melting peak in highly crosslinked samples was observed which is due to the fact that more than one type of PVDF crystals are present in these samples (1, 30).

Crystallization in a miscible blend consists of the diffusion of the crystallizable component towards the crystallization front and rejection of the non-crystallizable ingredient. The liquid-solid phase separation happening throughout the crystallization of PVDF in miscible dynamically vulcanized samples involves the segregation and diffusion of the amorphous vulcanized ACM away from the crystalline nucleus. The crosslinked ACM chains have a rather limited mobility compared with the linear polymer diluents.

Figure 9. shows Lorentz-corrected SAXS patterns and associated linear correlation functions (28) of 50/50-C1,C2 and C3 samples which have different crosslink density. Assuming the corresponding two-phase model, the average crystalline thickness (l_c), amorphous layer thickness (l_a), and the most probable value of long period (L) in the PVDF LS domains can be estimated via simple geometric analysis of $\gamma(x)$. Figure 10. shows these parameters obtained from the correlation function as a function of sulfur content for 50/50 and 40/60 samples with different crosslink density. The long period L and the amorphous layer thickness, $l_{a,}$ decreased with increasing the crosslink density. However this decrease is more pronounced for 50/50 and 40/60 blends compare to 20/80 sample. In contrast, the lamellar layer thickness l_c is almost insensitive to the crosslink density. Decreasing crystal long period and amorphous layer thickness again demonstrate the expulsion of ACM chains from amorphous layer of PVDF as a result of dynamic vulcanization induce phase separation. However, it seems that ACM chains in 20/80 samples do not follow the same trend to move out of the amorphous layer.

4. Discussion

From a thermodynamics point of view, increasing the molecular weight of one component of miscible blends can reduce the entropy of mixing and therefore induce phase decomposition; in this work, vulcanization of miscible blends was associated to the increase in the molecular weight of one of the components. Therefore, at least theoretically, dynamic vulcanization of a miscible blend must have the ability to induce the phase separation. PVDF/ACM blend is an interesting system to investigate this topic due to its unique phase diagram. The binodal curve of this system is skewed to PVDF rich side of phase diagram and therefore partially miscible blends (blends with more than 50% PVDF) are almost immiscible (19). The phase diagram of this system can be miscible and immiscible in various phase

compositions and temperatures therefore it allows us to compare both morphology and processability of different samples.

Dynamic vulcanization of immiscible blends is not a new subject of research and there are many reports in the literature(8-14). Dynamic vulcanization of immiscible PVDF/ACM samples showed a well-known morphology and torque behavior of these type of systems reported many times in the literature. But what is new about this work is some of the special phenomena observed in dynamic vulcanization of miscible blends i.e. nano-domain phase separated structure of 50/50-C1 and 40/60-C3 samples, complete phase separation upon increasing the crosslink density in 50/50-C3 system and miscibility of 20/80 systems even after dynamic vulcanization.

To explain these observations, 50/50-C1/220 sample was prepared. As mentioned in the results section ACM vulcanized droplets in 50/50-C1/220 sample are more than 400nm in diameter compared to 100nm droplets of 50/50-C1 sample. Furthermore, we noticed that while 50/50-C1/220 sample was melt processable, our effort to melting process the 50/50-C1 sample failed. Comparing SEM images and the processability of 50/50-C1 and 50/50-C1/220 samples, it can be concluded that at 220ºC system is completely phase separated while phase separation at 190ºC is imperfect. It then can be suggested that the polymer system is in binodal region at mixing condition for 50/50-C1 sample and nucleation and growth is the main mechanism of phase separation. Hence, system is at the early stage of nucleation which is the reason for observation of nano-domain phase separated. However, for 50/50-C1/220 sample nucleuses have grown significantly and phase separation is completed, which is associated to the bigger domains observed in inset of Figure 7.b.

Contrary to above a discussion which is mostly related to the liquid-liquid phase separation in melt state, SAXS results are related to the liquid-solid phase separation during the crystallization of PVDF. SAXS experiments showed that by increasing the crosslink density for 50/50 and 40/60 systems lamellar long period and amorphous layer thickness decreased while these parameters were unchanged for 20/80 system. Regarding this observation, it can be proposed that increasing the crosslink density increased the molecular weight of amorphous polymer and consequently shifted the phase diagram to the lower

temperatures at melt state. Therefore, in 50/50 and 40/60 systems which are near the boundary of phase separation, ACM chains have the ability to expel out of the crystal growth front and decreases the amorphous layer thickness. Nevertheless, 20/80 sample is deep into miscible region and due to a very slow diffusion of crosslinked ACM chains between the PVDF lamellae, phase separation does not happen. Therefore, the liquid-liquid phase separation facilitated the liquid-solid phase separation in 50/50 and 40/60 systems. This is not the case for 20/80 sample due to being fully miscible.

It is worth to mention that Figure 1. has been plotted at the quiescent condition, but in the mixer, blend is under complex flow filed of the rotating blades. Therefore, according to the Figure 1. at 205 ºC (working temperatures of mixer) 50/50 and 40/60 samples are completely into phase separated region, while as mentioned above they are fully miscible. Hence it suggests the presence of another important factor that has affected the system morphology and its processability and that is the effect of shear rate on system phase diagram at mixing condition. It seems that complex flow field of the Brabender mixer shifts the phase diagram to the higher temperatures. There are many reports in the literature on the effect of simple shear flow on phase miscibility/ immiscibility of the polymer blends (31-39), however, to the best of our knowledge it is the first time that the effect of shear rate at complex flow filed is reported. Figure 11. shows the schematic effects of the shear rate and crosslink density on the system phase diagram . According to our observation, in this system complex flow field of the mixer tends to enhance the miscible region while increasing the crosslink density which is related to the increase in the molecular weight tends to reduce the miscible region. Therefore, shear rate and crosslink density have played counter role in the dynamic condition during the mixing process. Given this hypothesis, interpretation of the behavior of the dynamically vulcanized PVDF/ACM system is very simple. Keeping this hypothesis in mind, Table 2 presents the observed morphology and processability of the system.

Dynamic vulcanization of PVDF/ACM blend has shown a very complex behavior. Three factors of dynamic vulcanization, flow filed (liquid-liquid phase separation) and crystallization (liquid-solid phase separation) play different roles in final morphology, crystal structure and processability of the system. It was not possible for us to weight each factor or separate their effects, however, further investigation of

this system using scientific equipment which provides in-situ analysis during melt mixing and dynamic vulcanization can provide valuable information on dynamic phase decomposition of macromolecular blends.

Conclusion

Effects of dynamic vulcanization on morphology, processability and crystalline structure of the partially miscible blend of PVDF/ACM were investigated. The resulted morphology was unique; dynamic vulcanization for samples near the phase separation boundary led to the nano-phase separated structure while samples deep into miscible region did not show any sign of phase separation. It was demonstrated that increasing the crosslink density induce phase separation by increasing the immiscible region and by rejection of ACM chains from PVDF lamellae when there is a strong drive for phase decomposition. Investigation of shear filed on phase decomposition showed that this parameter induce miscibility in the polymer system. It has been shown that three parameters of dynamic vulcanization, flow filed and crystallization are the main factors governing the morphology, processability and crystalline structure of the PVDF/ACM system.

References

1. Li Y, Oono Y, Kadowaki Y, Inoue T, Nakayama K, Shimizu H. A novel thermoplastic elastomer by reaction-induced phase decomposition from a miscible polymer blend. Macromolecules. 2006;39(12):4195-201.
2. Guo Q, Groeninckx G. Crystallization kinetics of poly (ε-caprolactone) in miscible thermosetting polymer blends of epoxy resin and poly (ε-caprolactone). Polymer. 2001;42(21):8647-55.
3. Guo Q, Harrats C, Groeninckx G, Koch M. Miscibility, crystallization kinetics and real-time small-angle X-ray scattering investigation of the semicrystalline morphology in thermosetting polymer blends of epoxy resin and poly (ethylene oxide). Polymer. 2001;42(9):4127-40.
4. Guo Q, Harrats C, Groeninckx G, Reynaers H, Koch M. Miscibility, crystallization and real-time small-angle X-ray scattering investigation of the semicrystalline morphology in thermosetting polymer blends. Polymer. 2001;42(14):6031-41.
5. Zheng S, Zheng H, Guo Q. Epoxy resin/poly (ϵ-caprolactone) blends cured with 2, 2-bis [4-(4-aminophenoxy) phenyl] propane. I. Miscibility and crystallization kinetics. Journal of Polymer Science Part B: Polymer Physics. 2003;41(10):1085-98.

6. Guo Q, Thomann R, Gronski W, Thurn-Albrecht T. Phase Behavior, Crystallization, and Hierarchical Nanostructures in Self-Organized Thermoset Blends of Epoxy Resin and Amphiphilic Poly (ethylene oxide)-b lock-poly (propylene oxide)-b lock-poly (ethylene oxide) Triblock Copolymers. Macromolecules. 2002;35(8):3133-44.
7. l'Abee RMA, Goossens JGP, van Duin M. Thermoplastic Vulcanizates by Reaction-Induced Phase Separation of a Miscible Poly(ϵ-Caprolactone)/Epoxy System. Rubber chemistry and technology. 2007;80(2):311-23.
8. Goharpey F, Nazockdast H, Katbab A. Relationship between the rheology and morphology of dynamically vulcanized thermoplastic elastomers based on EPDM/PP. Polymer Engineering & Science. 2005;45(1):84-94.
9. Naderi G, Lafleur PG, Dubois C. Microstructure-properties correlations in dynamically vulcanized nanocomposite thermoplastic elastomers based on PP/EPDM. Polymer Engineering & Science. 2007;47(3):207-17.
10. Prut E, Erina N, Karger-Kocsis J, Medintseva T. Effects of blend composition and dynamic vulcanization on the morphology and dynamic viscoelastic properties of PP/EPDM blends. Journal of Applied Polymer Science. 2008;109(2):1212-20.
11. Abdou-Sabet S, Puydak R, Rader C. Dynamically vulcanized thermoplastic elastomers. Rubber chemistry and technology. 1996;69(3):476-94.
12. Uthaipan N, Junhasavasdikul B, Nakason C, Thitithammawong A. Assessment of Mixing Efficiency of Intermeshing Rotor Mixers on Morphological and Mechanical Properties and Crosslink Density of Dynamically Vulcanized EPDM/PP Blends. Advanced Materials Research. 2014;844:122-6.
13. Wu H, Ning N, Zhang L, Tian H, Wu Y, Tian M. Effect of additives on the morphology evolution of EPDM/PP TPVs during dynamic vulcanization in a twin-screw extruder. Journal of Polymer Research. 2013;20(10):1-8.
14. Babu RR, Naskar K. Recent developments on thermoplastic elastomers by dynamic vulcanization. Advanced Rubber Composites: Springer; 2011. p. 219-47.
15. Chen Y, Xu C, Cao L, Wang Y, Fang L. Morphology Study of Peroxide-Induced Dynamically Vulcanized Polypropylene/Ethylene-Propylene-Diene Monomer/Zinc Dimethacrylate Blends during Tensile Deformation. The Journal of Physical Chemistry B. 2013;117(25):7819-25.
16. Ramanujam A, Kim K, Kyu T. Phase diagram, morphology development and vulcanization induced phase separation in blends of syndiotactic polypropylene and ethylene–propylene diene terpolymer. Polymer. 2000;41(14):5375-83.
17. Li Y, Oono Y, Nakayama K, Shimizu H, Inoue T. Dual lamellar crystal structure in poly (vinylidene fluoride)/acrylic rubber blends and its biaxial orientation behavior. Polymer. 2006;47(11):3946-53.
18. Abolhasani M, Jalali-Arani A, Nazockdast H, Guo Q. Poly (vinylidene fluoride)-acrylic rubber partially miscible blends: Crystallization within conjugated phases induce dual lamellar crystalline structure. Polymer. 2013;54(17):4686-701.
19. Abolhasani MM, Guo Q, Jalali-Arani A, Nazockdast H. Poly(vinylidene fluoride)–acrylic rubber partially miscible blends: Phase behavior and its effects on the mechanical properties. Journal of Applied Polymer Science. 2013;130(2):1247-58.
20. Imken R, Paul D, Barlow J. Transition behavior of poly (vinylidene fluoride)/poly (ethyl methacrylate) blends. Polymer Engineering & Science. 1976;16(9):593-601.
21. Penning J, St. John Manley R. Miscible blends of two crystalline polymers. 2. Crystallization kinetics and morphology in blends of poly (vinylidene fluoride) and poly (1, 4-butylene adipate). Macromolecules. 1996;29(1):84-90.
22. Rahman MH, Nandi AK. Miscibility and crystallization behavior of poly (ethylene terephthalate)/poly (vinylidene fluoride) blends. Macromolecular Chemistry and Physics. 2002;203(4):653-62.

23. Bernstein R, Paul D, Barlow J. Polymer blends containing poly (vinylidene fluoride). Part II: Poly (vinyl esters). Polymer Engineering & Science. 1978;18(9):683-6.
24. Lovinger AJ. Poly (vinylidene fluoride). Developments in Crystalline Polymers—1: Springer; 1982. p. 195-273.
25. Nishi T, Wang T. Melting point depression and kinetic effects of cooling on crystallization in poly (vinylidene fluoride)-poly (methyl methacrylate) mixtures. Macromolecules. 1975;8(6):909-15.
26. Morra BS, Stein RS. Melting studies of poly (vinylidene fluoride) and its blends with poly (methyl methacrylate). Journal of Polymer Science: Polymer Physics Edition. 1982;20(12):2243-59.
27. Glatter O, Kratky O. Small angle X-ray scattering: Academic press London; 1982.
28. Strobl G, Schneider M, Voigt-Martin I. Model of partial crystallization and melting derived from small-angle X-ray scattering and electron microscopic studies on low-density polyethylene. Journal of Polymer Science: Polymer Physics Edition. 1980;18(6):1361-81.
29. Tang Y, Lu K, Cao X, Li Y. Nanostructured Thermoplastic Vulcanizates by Selectively Cross-Linking a Thermoplastic Blend with Similar Chemical Structures. Industrial & Engineering Chemistry Research. 2013;52(35):12613-21.
30. Abolhasani MM, Naebe M, Jalali-Arani A, Guo Q. Influence of Miscibility Phenomenon on Crystalline Polymorph Transition in Poly (Vinylidene Fluoride)/Acrylic Rubber/Clay Nanocomposite Hybrid. PLOS ONE. 2014;9(2):e88715.
31. Zou F, Dong X, Liu W, Yang J, Lin D, Liang A, et al. Shear Induced Phase Boundary Shift in the Critical and Off-Critical Regions for a Polybutadiene/Polyisoprene Blend. Macromolecules. 2012;45(3):1692-700.
32. Samuel C, Raquez J-M, Dubois P. PLLA/PMMA blends: a shear-induced miscibility with tunable morphologies and properties? Polymer. 2013.
33. Shi W, Yang J, Liu W, Zhang L, Han CC. Anomalous Phase Separation Dynamics under Asymmetric Viscoelastic Effect: Where Fluidic and Elastic Properties Meet. Macromolecules. 2013;46(6):2516-20.
34. Lin D, Cheng H, Zou F, Ning W, Han CC. Morphology evolution of a bisphenol A polycarbonate/poly (styrene-< i> co</i>-acrylonitrile) blend under shear and after shear cessation. Polymer. 2012;53(6):1298-305.
35. Horst R, Wolf B. Calculation of the phase separation behavior of sheared polymer blends. Macromolecules. 1992;25(20):5291-6.
36. Hindawi I, Higgins J, Weiss R. Flow-induced mixing and demixing in polymer blends. Polymer. 1992;33(12):2522-9.
37. Yu W, Li R, Zhou C. Rheology and phase separation of polymer blends with weak dynamic asymmetry. Polymer. 2011;52(12):2693-700.
38. Yeganeh JK, Goharpey F, Foudazi R. Can only rheology be used to determine the phase separation mechanism in dynamically asymmetric polymer blends (PS/PVME)? RSC Advances. 2012;2(21):8116-27.
39. Chen F, Zhang J. Effects of Plasticization and Shear Stress on Phase Structure Development and Properties of Soy Protein Blends. ACS Applied Materials & Interfaces. 2010;2(11):3324-32.

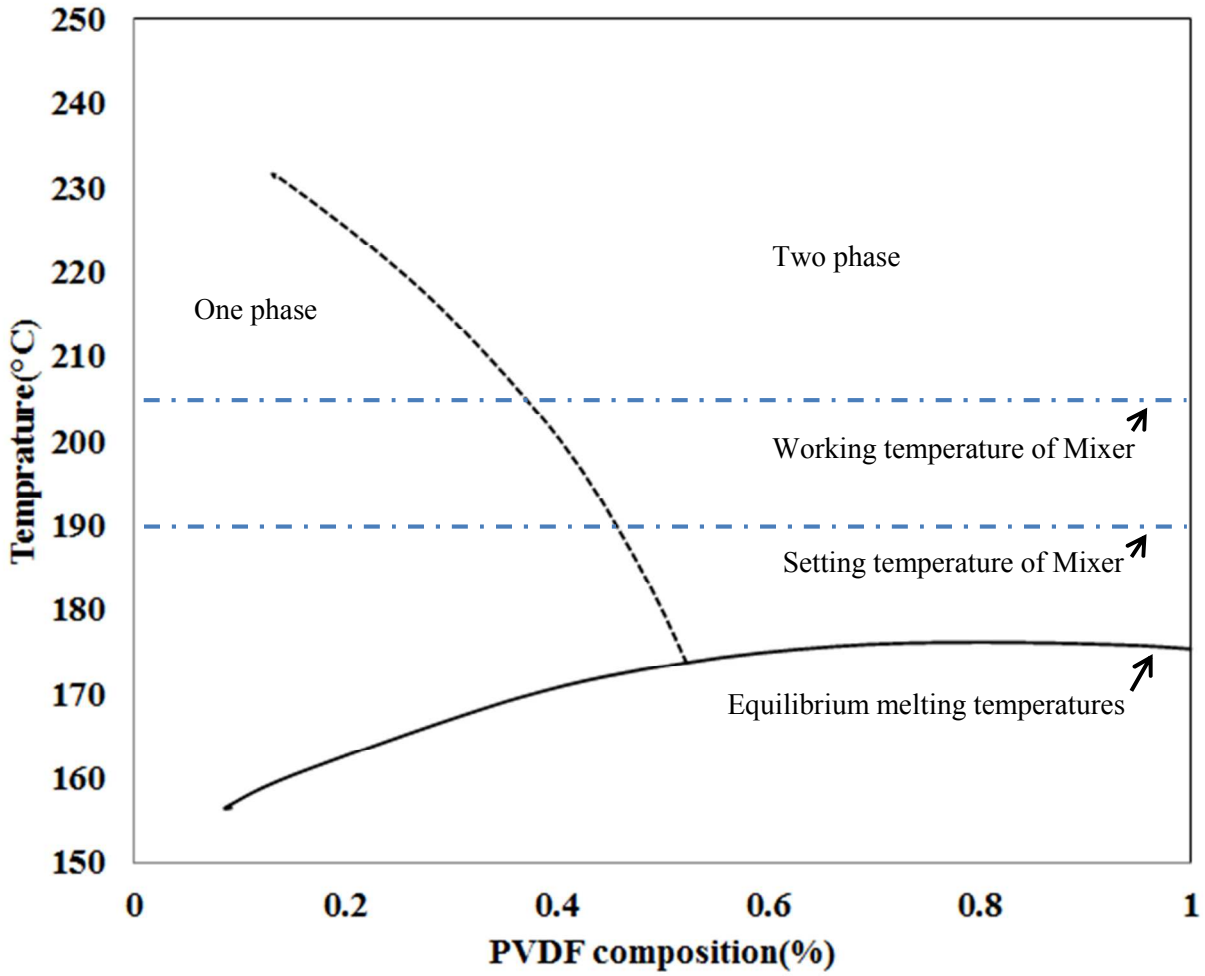

Figure 1. Phase diagram of PVDF/ACM blends in quiescent condition.

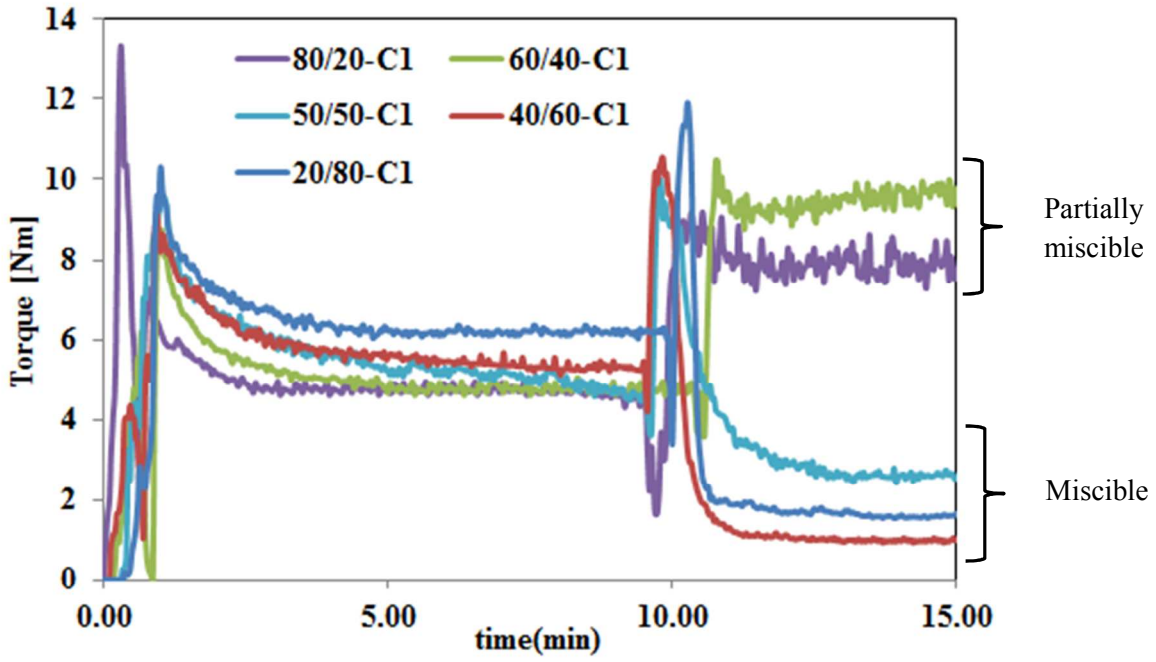

Figure 2. Mixing torque vs mixing time for dynamically vulcanized samples with 1phr sulfur.

Figure 3. photograph of a) 80/20-C1, b) 50/50-C3, c) 50/50-C1/220, d) 50/50-C2, e)20/80-C1 and f)20/80-C3 after dynamic vulcanization.

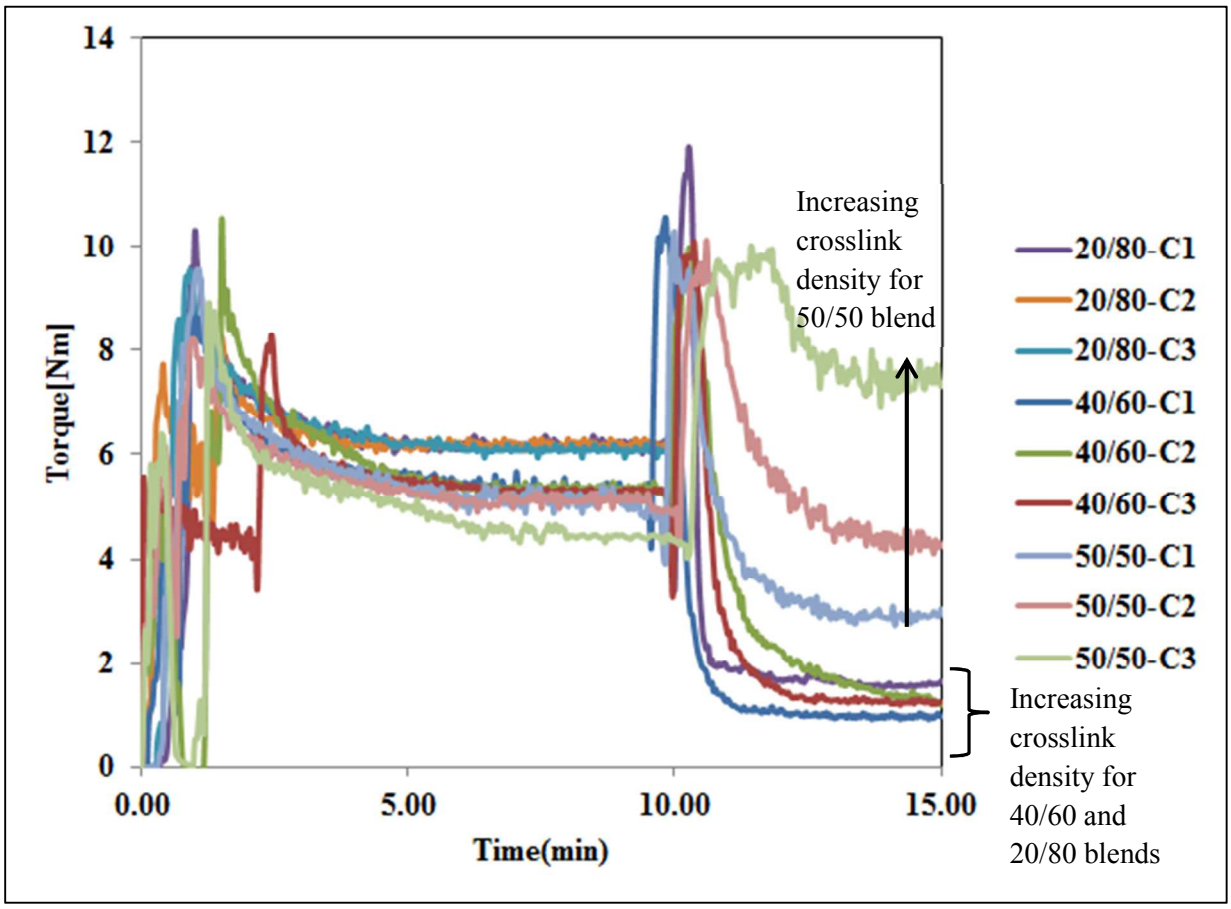

Figure 4. Mixing torque vs mixing time for dynamically vulcanized miscible blends with various crosslink densities.

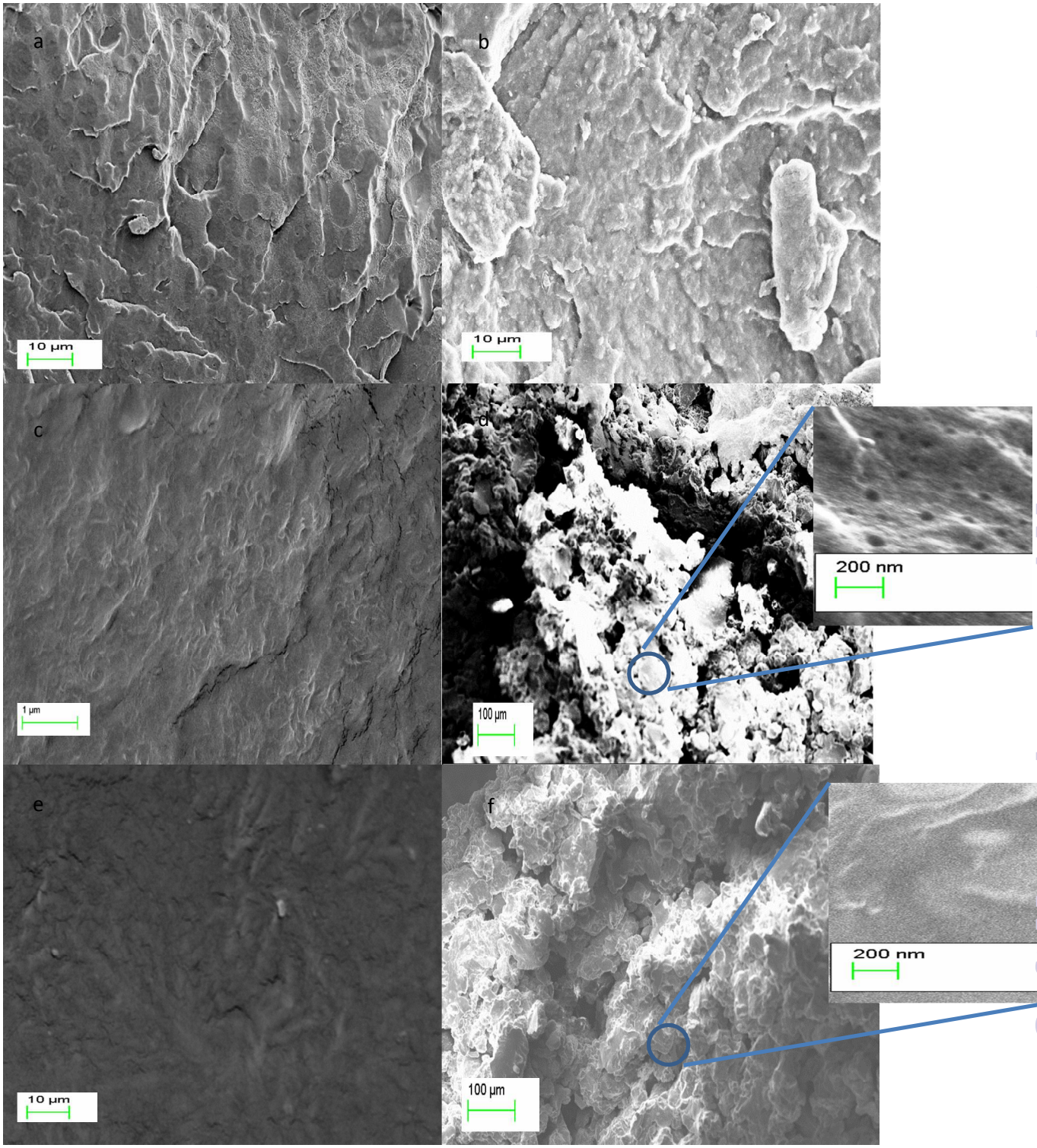

Figure 5. SEM micrographs of different miscible and partially miscible samples before and after dynamic vulcanization with 1 phr sulfur a)80/20 sample, b) 80/20-C1 sample, C)50/50 sample, d)50/50-C1 sample, e) 20/80 sample, f) 20/80-C1 sample. Insets show higher magnification photos.

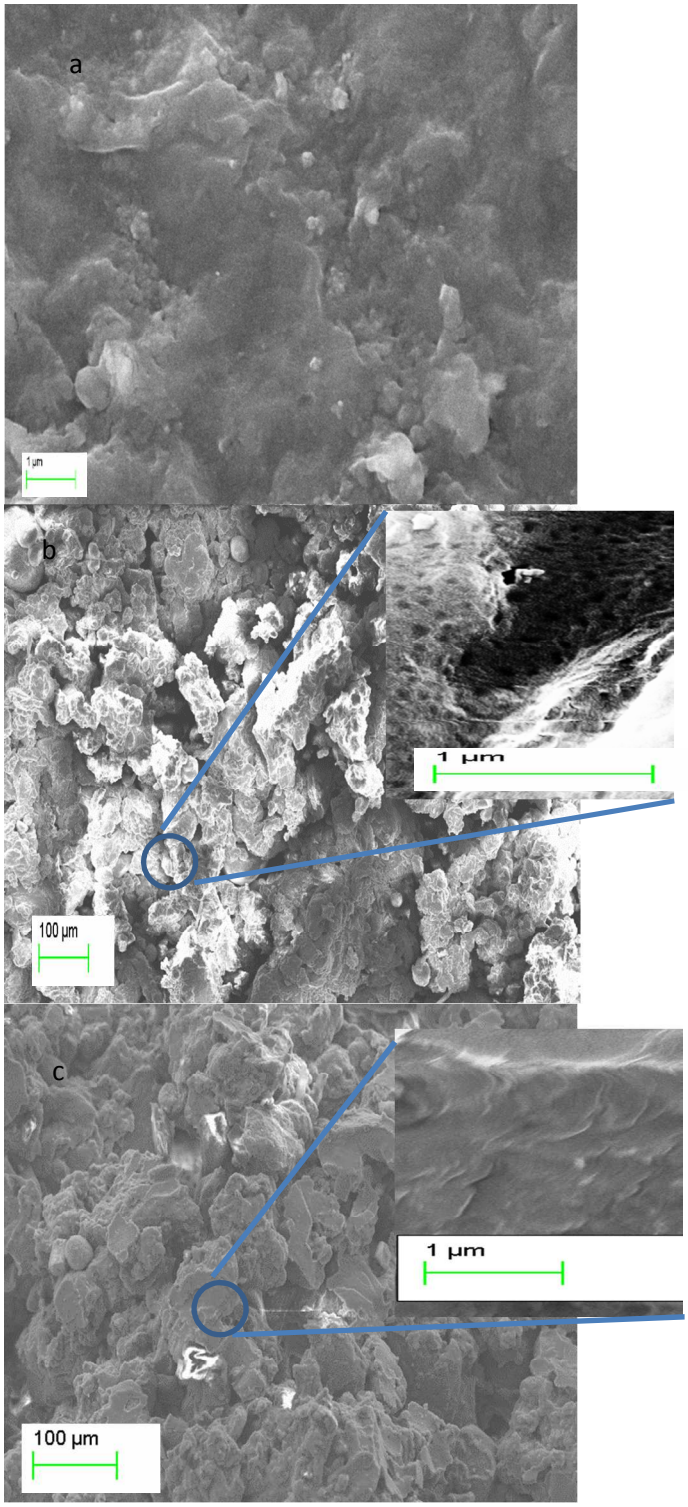

Figure 6. SEM micrographs of miscible samples dynamic vulcanization with 3 phr sulfur with different magnification a)50/50-C3 sample, b) 40/60-C3 sample, C)20/80-C3 sample. Insets show higher magnification photos.

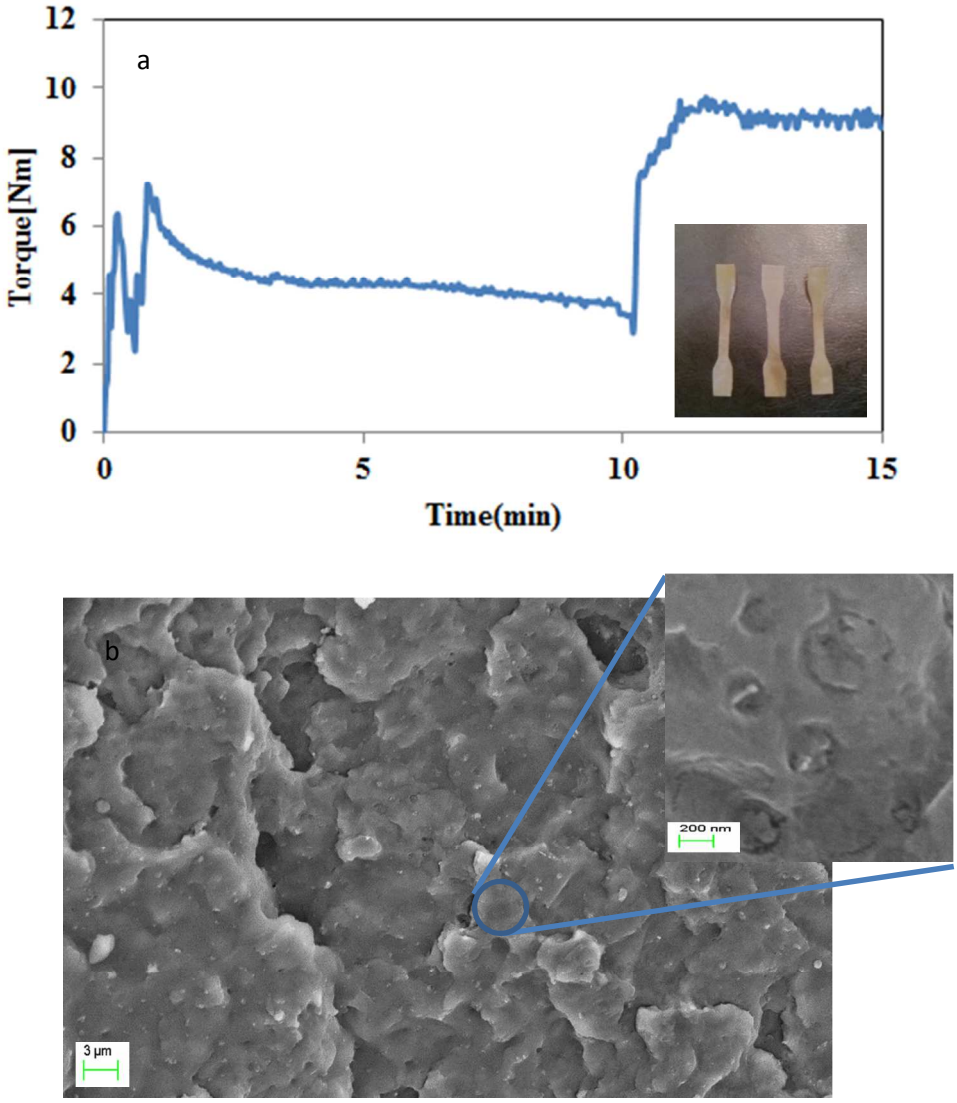

Figure 7. 50/50 blend dynamically vulcanized at 220°C with 1phr sulfur (50/50-C1/220 sample) a) Mixing torque vs mixing time b) SEM images

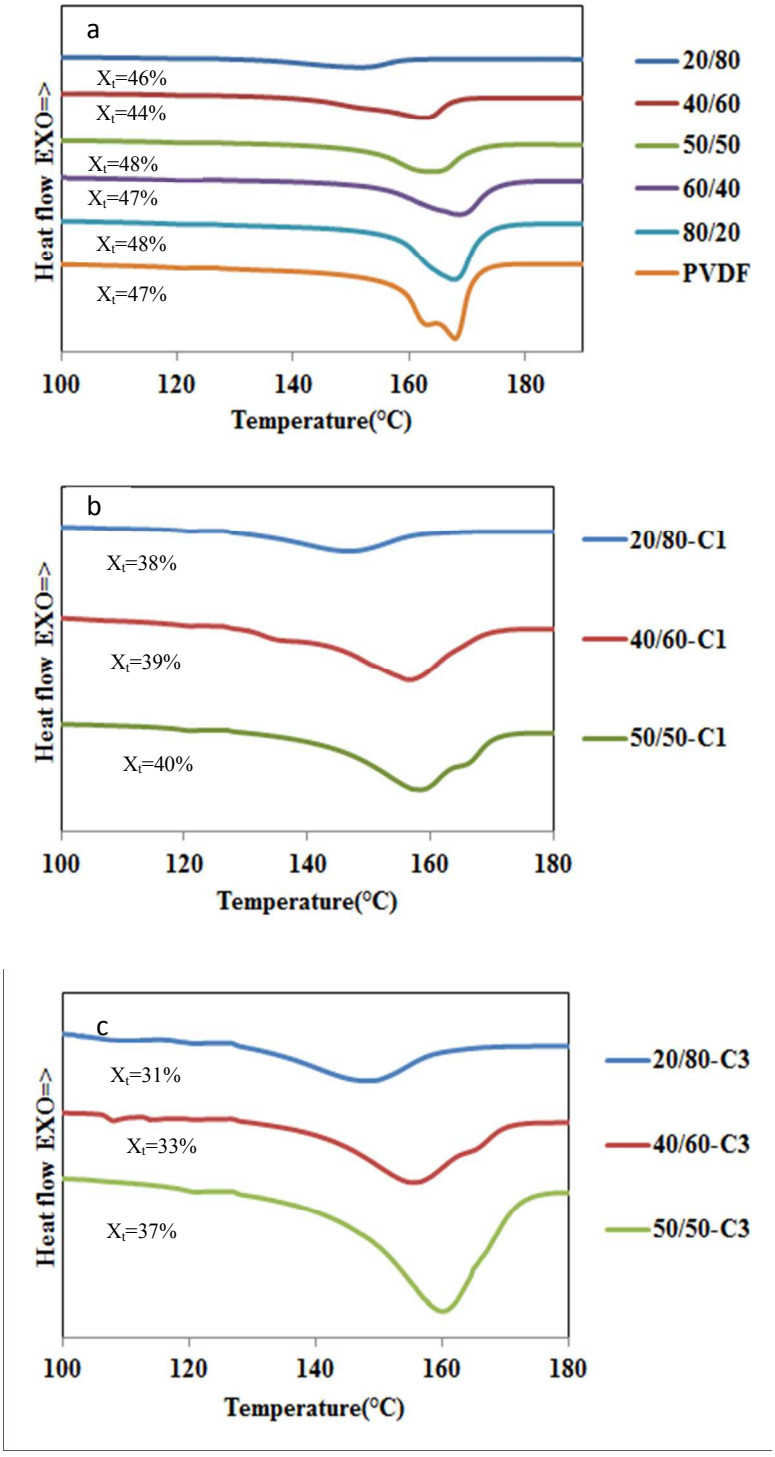

Figure 8. DSC thermograms of a) PVDF/ACM blends, b) PVDF/ACM miscible blends after dynamic vulcanization with 1phr sulfur, c) PVDF/ACM miscible blends after dynamic vulcanization with 3phr sulfur, at the heating rate of 10°C/min.

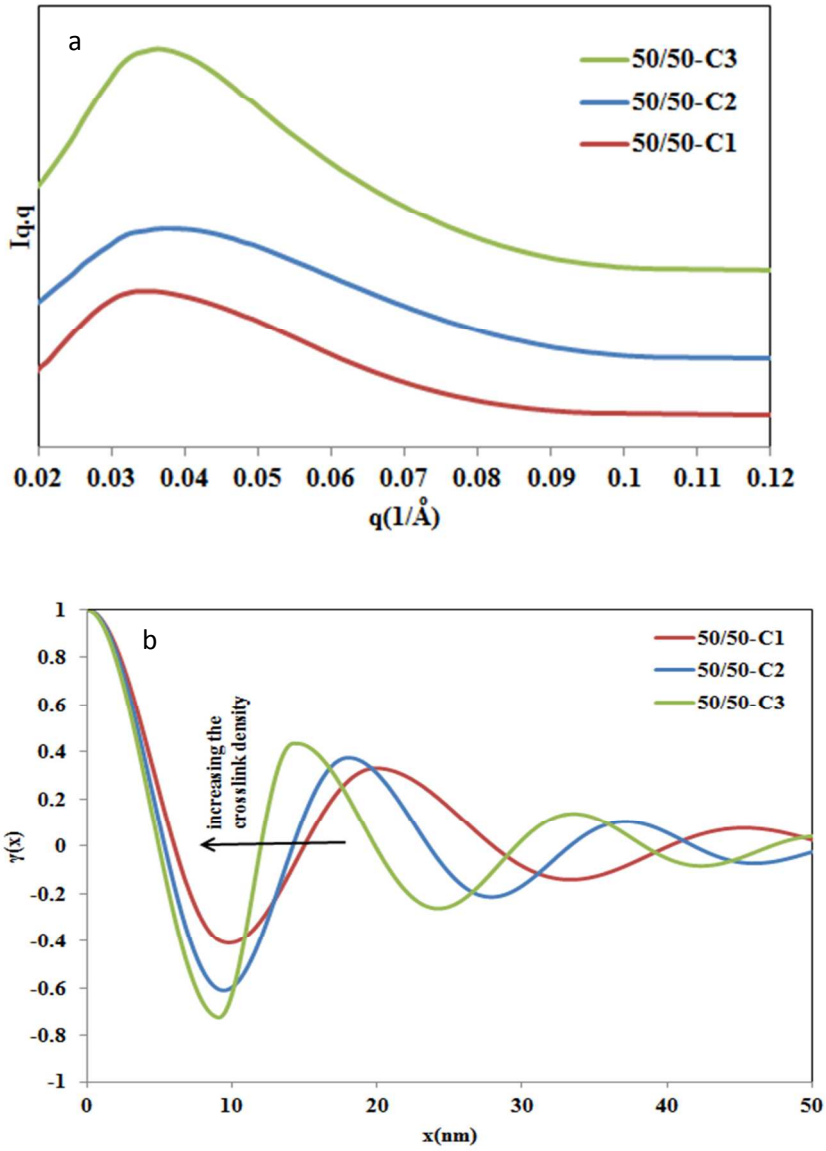

Figure 9. a) Lorentz corrected SAXS patterns of 50/50 sample with different crosslink density, b) linear correlation functions for of 50/50 sample with different crosslink density.

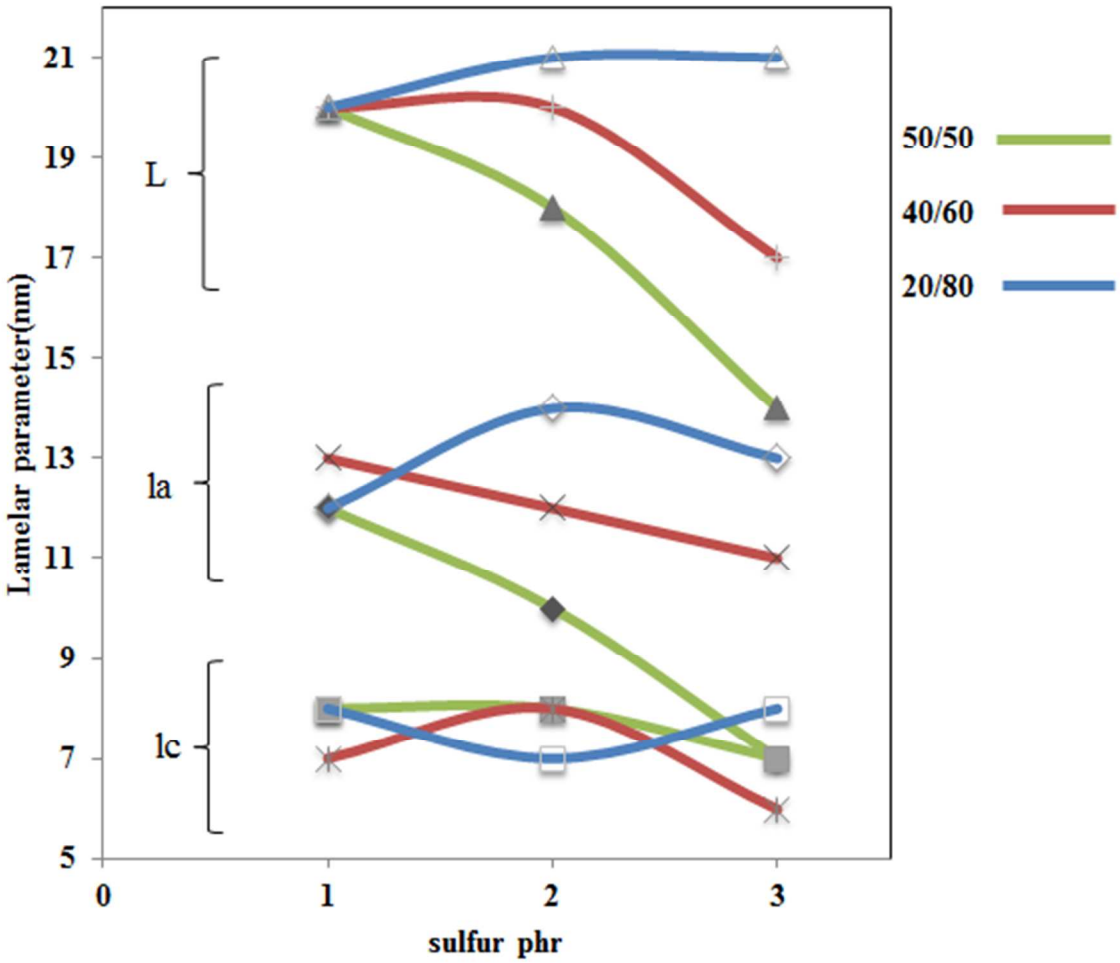

Figure 10. Variations of lamellar parameters as a function of crosslink density for miscible samples of 50/50 filed symbols(▲♦■), 40/60 cross symbols(+×□) and 20/80 open symbols(Δ◊□).

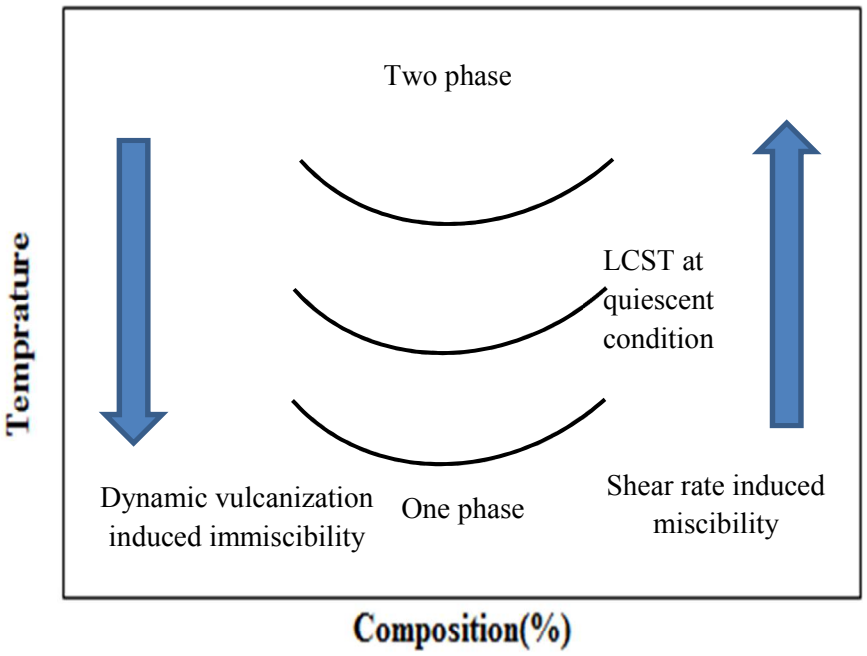

Figure 11. Schematic effects of Shear rate and crosslink density on phase diagram of PVDF/ACM blend

Table 1. Details of prepared samples

Sample	PVDF(wt%)	ACM(wt%)	Sulfur(phr)	Brabender setting temperature(°C)
PVDF	100	0	0	190°C
80/20	80	20	0	190°C
60/40	60	40	0	190°C
50/50	50	50	0	190°C
40/60	40	60	0	190°C
20/80	20	80	0	190°C
80/20-C1	80	20	1	190°C
60/40-C1	60	40	1	190°C
50/50-C1	50	50	1	190°C
40/60-C1	40	60	1	190°C
20/80-C1	20	80	1	190°C
50/50-C2	50	50	2	190°C
40/60-C2	40	60	2	190°C
20/80-C2	20	80	2	190°C
50/50-C3	50	50	3	190°C
40/60-C3	40	60	3	190°C
20/80-C3	20	80	3	190°C
50/50-C1/220	50	50	1	220°C

Table 2. Summary of torque and related morphology for samples studied.

sample	Brabender mixer setting temperature	Miscibility statue of the initial PVDF/ACM blends (without curative) at quiescent condition at room temperature	Torque status after addition of curatives	Melt processability	Observed morphology
80/20-C1	190ºC	Partially miscible	increased	YES	Vulcanized ACM domains in PVDF matrix
60/40-C1	190ºC	Partially miscible	increased	YES	Vulcanized ACM domains in PVDF matrix
50/50-C1	190ºC	Miscible	decreased	NO	nanometer droplets of ACM were phase separated
40/60-C1	190ºC	Miscible	decreased	NO	porous structure
20/80-C1	190ºC	Miscible	decreased	NO	porous structure
50/50-C3	190ºC	Miscible	increased	YES	Vulcanized ACM domains in PVDF matrix
40/60-C3	190ºC	Miscible	decreased	NO	nanometer droplets of ACM were phase separated
20/80-C3	190ºC	Miscible	decreased	NO	porous structure
50/50-C1	220ºC	Miscible	increased	YES	Submicron vulcanized ACM domains in PVDF matrix